Progress towards an accuracy evaluation of NIST-F4 cesium fountain clock

Vladislav Gerginov
Time and Frequency Division
National Institute of Standards and Technology
Boulder, CO, USA
Vladislav.Gerginov@nist.gov

Gregory W. Hoth
Time and Frequency Division
National Institute of Standards and Technology
Boulder, CO, USA
Gregory.Hoth@nist.gov

Thomas P. Heavner
Time and Frequency Division
National Institute of Standards and Technology
Boulder, CO, USA
Thomas.Heavner@nist.gov

Jeff A. Sherman
Time and Frequency Division
National Institute of Standards and Technology
Boulder, CO, USA
Jeffrey.Sherman@nist.gov

***Abstract*—This work presents preliminary results towards the evaluation of the NIST-F4 cesium primary frequency standard. We present measurements of NIST-F4 frequency instability and evaluation of some of its systematic frequency shifts and shift uncertainties.**

Keywords—atomic fountain clocks, primary frequency references, frequency metrology

2024 European Frequency and Time Forum (EFTF) | 979-8-3503-5427-0/24/$31.00 USG | DOI: 10.1109/EFTF61992.2024.10722735

I. Introduction

Cesium atomic fountain clocks [1] are the most accurate primary frequency standards, some reaching frequency instabilities below the $10^{-13}/\sqrt{\tau}$ level (with τ the measurement time in seconds) and accuracies at the low-10^{-16} level [2-5]. Such performance requires careful evaluation and correction for multiple effects leading to frequency shifts. We report preliminary analysis of the NIST-F4 frequency instability and present evaluation of the quadratic Zeeman, blackbody radiation, and collisional frequency shifts and their uncertainties.

II. Brief description of NIST-F4

NIST-F4 uses optical molasses cooling of cesium atoms [1]. A Ti:Sapphire laser provides light for laser cooling and detection, and a Distributed Bragg Reflector laser provides repumping light. The vertically launched atom cloud passes through a set of microwave cavities for atom state preparation and Ramsey sequence interrogation. The microwaves are generated from an Oven Controlled Crystal Oscillator (OCXO) phase-locked to one of NIST's hydrogen masers using a home-built microwave synthesizer [6]. The microwave synthesizer supports a short-term instability of approximately 10^{-13} at one second, determined by the phase noise of the OCXO. In normal operation, NIST-F4 uses three independent frequency servos for frequency measurements, atomic collisional shift estimation using high- and low-density cloud configurations, and bias magnetic field frequency measurement for online monitoring of the quadratic Zeeman frequency shift of the clock transition. In-vacuum temperature measurements of the structure surrounding the atoms provide information about the blackbody radiation (BBR) shift experienced by the atoms during a measurement campaign.

III. Frequency evaluation

During a frequency evaluation, the control program of NIST-F4 [7] modulates and tunes a 7.368 MHz frequency synthesizer in the microwave synthesizer chain to bring the mixed 9.192 GHz microwave frequency to resonance with the cesium clock transition (for high- and low-density modes of operation) or to a magnetically sensitive microwave transition (for magnetic field measurement). The control program alternates the servos in a duty cycle that minimizes the frequency measurement uncertainties and tracks possible drifts in the bias magnetic field. The fountain frequency instability in high- and low-density operation is determined by roughly equal contributions from OCXO phase noise and detection noise. The detection noise is dominated by quantum projection noise resulting from the limited number of detected atoms [1]. The servo that tracks the frequency of the magnetically sensitive microwave transition is activated approximately once an hour and determines the transition frequency to within ± 0.1 Hz in less than 30 s.

IV. Microwave cavities

The identical state selection and Ramsey microwave cavities of NIST-F4 [8] were machined from oxygen-free copper. The Ramsey cavity (see Fig. 1) has a Q-factor of 2.85×10^4, 10 percent below a prediction by finite element simulations [9]. The microwave field in the cavity can be delivered via four independent feeds for suppressing distributed cavity phase (DCP) shifts [10].

A portion of the microwave-feed network for balancing the four independent feeds in amplitude and phase is shown in Fig. 2. The microwave-feed distribution network allows us to equalize the microwave amplitudes to below 0.1 dB and the

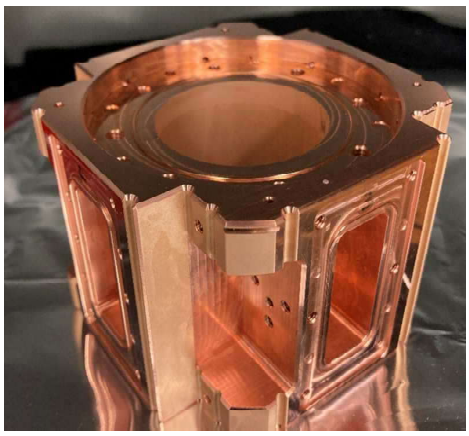

Figure 1. Body of the Ramsey microwave cavity. For scale, the diameter of the central bore is 43 mm.

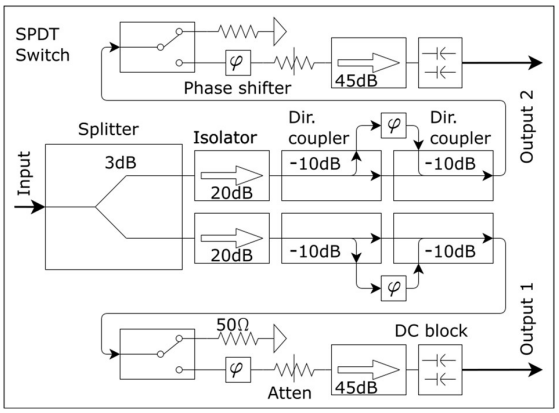

Figure 2. Microwave-feed network for two feeds. A copy of this system is used to drive the other two feeds for the Ramsey cavity.

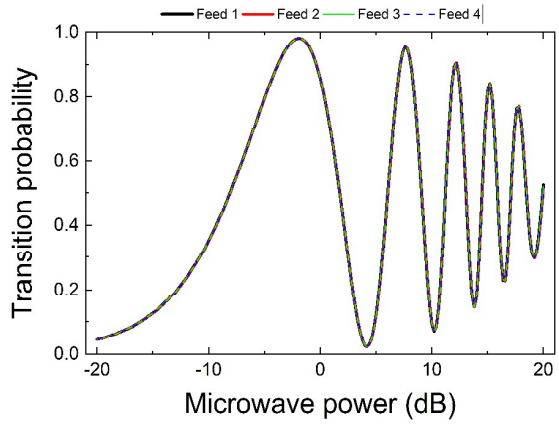

Figure 3. Transition probability as a function of microwave power for each individual feed after balancing each arm in the network by fine-tuning the attenuation. The maximum difference in transition probability between the four feeds shown is 0.027 over the full scan. Near normal operating power (first maximum), the transition probability due to individual feeds agree to better than 0.005.

microwave phases to below 100 μrad. The amplitude is balanced by measuring the Rabi flopping of the atomic transition probability resulting from activating feeds one at a time and scanning the output power of the Ramsey microwave synthesizer, as shown in Figure 3.

V. Frequency Instability

In high-density mode, we measure an instability of $1.6 \times 10^{-13}/\sqrt{\tau}$, limited partially by detection noise and partially by the phase noise of the OCXO-based local oscillator [6]. By driving the microwave chain with a photonic oscillator [11], we achieved a short-term frequency instability of $1.1 \times 10^{-13}/\sqrt{\tau}$ up to $\tau = 20$ s. At longer averaging times, the drift of the free-running photonic LO begins to limit the frequency stability.

At short averaging times, the phase noise of the photonic oscillator is more than an order of magnitude better than the OCXO, so this experiment allows us to cleanly separate the phase noise due to our usual local oscillator from the fountain detection noise. Measurements of the Allan deviation, $\sigma_y(\tau)$, of the fountain operating in high-density mode using the OCXO (red symbols) and using the photonic oscillator (green symbols) are shown in Figure 4.

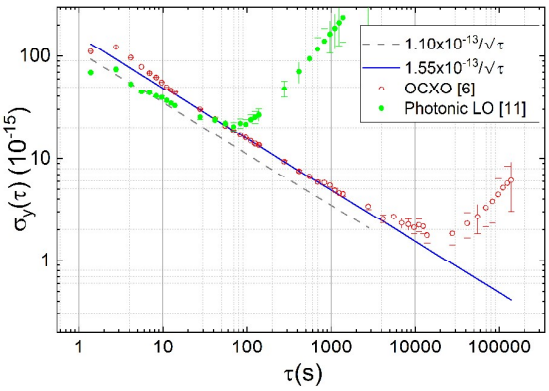

Figure 4. Allan deviation using OCXO phase-locked to a hydrogen maser (red open symbols) and the free-running photonic oscillator (solid green symbols). The drift visible in the data taken with the OCXO after 10^4 s is due to the hydrogen maser which provides the frequency reference for the fountain synthesis chain [6].

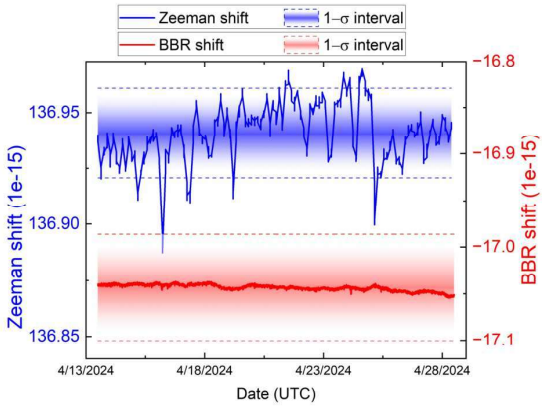

Figure 5. Typical variation of the quadratic Zeeman and blackbody radiation shifts as a function of time. The 1-σ intervals and the mean value of each shift over the measurement campaign are indicated by the shaded region and the dashed lines. The 1-σ intervals combine statistical and systematic uncertainties. For the Zeeman shift, the two components of the uncertainty have similar magnitude. For the BBR shift, the uncertainty is dominated by the systematic component due to the preliminary estimate of the temperature sensor accuracy.

VI. Collisional Shift

The measured frequency difference between the two modes of operation, as well as the detected total atom numbers are used to quantify the atomic collisional shift as a function of the total atom number assuming that the shift depends linearly on the detected atom number [1]. The collisional shift in high-density is typically at the 1×10^{-15} level. A 10 percent systematic uncertainty is assigned to the shift value.

VII. Quadratic Zeeman and Blackbody Radiation Shifts

During a frequency evaluation campaign, the magnetic field inside the fountain and the temperature of the apparatus must be monitored to correct for the quadratic Zeeman shift and the blackbody radiation shift. Typical shifts observed in a recent measurement campaign are shown in Fig. 5.

The fountain control software performs frequency measurements of the magnetically sensitive microwave transition $|F = 3, m_F = -1 \rightarrow F = 4, m_F = -1\rangle$, providing information about the average bias magnetic field experienced by the atoms. The measurement instability and the field

inhomogeneity along the atomic cloud trajectory lead to a quadratic Zeeman shift uncertainty of 2×10^{-17} [12].

The ambient temperature is periodically measured with an in-vacuum calibrated platinum resistance temperature detector (PT100). The sensor is mounted in vacuum on the drift tube of the fountain. A preliminary, conservative estimate of the temperature measurement accuracy of 0.2 K results in a blackbody shift uncertainty of 6×10^{-17} [13-14].

ACKNOWLEDGMENT

The authors acknowledge the technical help from Dr. Johannes Rahm and Dr. Stefan Weyers (Physikalisch-Technische Bundesanstalt, Germany) with the fountain control software, and of the instrument makers Hans Green, Calvin Schwadron, Adam Ellzey, James Uhrich, and Kyle Thatcher (JILA, USA) with the design and fabrication of the NIST-F4 microwave cavities. This work was funded by NIST, a U.S. government agency. It is not subject to copyright.

REFERENCES

[1] R. Wynands and S. Weyers, "Atomic fountain clocks", Metrologia 42, S64, 2005.

[2] M. Abgrall *et al.*, "Atomic fountains and optical clocks at SYRTE: Status and perspectives," Comptes Rendus Physique, vol. 16, no. 5, pp. 461–470, 2015.

[3] S. Weyers *et al.*, "Advances in the accuracy, stability, and reliability of the PTB primary fountain clocks," Metrologia, vol. 55, no. 6, p. 789, 2018.

[4] K. Szymaniec, S. N. Lea, K. Gibble, S. E. Park, K. Liu, and P. Glowacki, "NPL Cs fountain frequency standards and the quest for the ultimate accuracy," Journal of Physics: Conference Series, vol. 723, no. 1, p. 012003, 2016.

[5] S. Beattie *et al.*, "First accuracy evaluation of the NRC-FCs2 primary frequency standard," Metrologia, vol. 57, no. 3, p. 035010, 2020.

[6] T. Heavner, S. Jefferts, E. Donley, T. Parker, and F. Levi, "A new microwave synthesis chain for the primary frequency standard NIST-F1," in Proceedings of the 2005 IEEE International Frequency Control Symposium and Exposition, pp. 308–311. 2005.

[7] Courtesy of Dr. J. Rahm and Dr. S. Weyers from Physikalisch-Technische Bundesanstalt (PTB), Germany.

[8] V. Gerginov *et al., unpublished.*

[9] G. W. Hoth, B. Patla, N. Ashby, and V. Gerginov, Proc. Joint Mtg. IEEE Intl. Freq. Cont. Symp. and EFTF Conf., 2022.

[10] R. Li and K. Gibble, Metrologia 47 534, 2010.

[11] Using a free-running photonic oscillator from Menlo Systems GmbH. Any mention of commercial products is for information only; it does not imply recommendation or endorsement by NIST.

[12] J. Vanier and C. Audoin, The Quantum Physics of Atomic Frequency Standards. Institute of Physics Publishing, 1989.

[13] P. Rosenbusch, S. Zhang, and A. Clairon, "Blackbody radiation shift in primary frequency standards," in IEEE International Frequency Control Symposium Joint with the 21st European Frequency and Time Forum, 2007, pp. 1060–1063, 2007.

[14] E. J. Angstmann, V. A. Dzuba, and V. V. Flambaum, "Frequency shift of hyperfine transitions due to blackbody radiation," Phys. Rev. A, vol. 74, p. 023405, 2006.